Draft version February 5, 2008
Preprint typeset using LaTeX style emulateapj v. 10/09/06

THE TAIWANESE-AMERICAN OCCULTATION SURVEY: THE MULTI-TELESCOPE ROBOTIC OBSERVATORY

M. J. Lehner[1,2], C.-Y. Wen[1], J.-H. Wang[1], S. L. Marshall[3,4], M. E. Schwamb[5], Z.-W. Zhang[6], F. B. Bianco[7,2], J. Giammarco[8], R. Porrata[9], C. Alcock[2], T. Axelrod[10], Y.-I. Byun[11], W. P. Chen[5], K. H. Cook[4], R. Dave[12], S.-K. King[1], T. Lee[1], H.-C. Lin[5] and S.-Y. Wang[1]

Draft version February 5, 2008

ABSTRACT

The Taiwanese-American Occultation Survey (TAOS) operates four telescopes to search for occultations of stars by Kuiper Belt Objects. This paper provides a detailed description of the TAOS multi-telescope system.

Subject headings: Solar System, Astronomical Instrumentation, Astronomical Techniques

1. INTRODUCTION

The Taiwanese American Occultation Survey (TAOS) continuously monitors up to ∼1,000 stars with four telescopes at 5 Hz, for the purpose of detecting occultations of these stars by small ($\gtrsim$1 km) objects in the Kuiper Belt and beyond. Installation of the first three telescopes and the first version of the control software were completed in January 2005, and the survey was officially started shortly thereafter. Installation of the fourth telescope was completed in January 2007, and four telescope operations commenced in April, 2008.

The principal science questions we plan to address with this survey are:

- What is the number and size distribution of small (∼1–10 km in diameter) bodies in the trans-Neptunian region?

- Is there an extension of the Kuiper Belt beyond 50 AU comprising bodies too small to have been detected in direct surveys?

- What is the number and size distribution of objects (e.g. Sedna) in the *Extended Disk* of the Solar System?

Electronic address: mlehner@asiaa.sinica.edu.tw
[1] Institute of Astronomy and Astrophysics, Academia Sinica. P.O. Box 23-141, Taipei 106, Taiwan
[2] Harvard-Smithsonian Center for Astrophysics, 60 Garden Street, Cambridge, MA 02138
[3] Kavli Institute for Particle Astrophysics and Cosmology, 2575 Sand Hill Road, MS 29, Menlo Park, CA 94025
[4] Institute for Geophysics and Planetary Physics, Lawrence Livermore National Laboratory, Livermore, CA 94550
[5] Department of Astronomy, California Institute of Technology, 1201 E. California Blvd., Pasadena, CA 91125
[6] Institute of Astronomy, National Central University, No. 300, Jhongda Rd, Jhongli City, Taoyuan County 320, Taiwan
[7] Department of Physics and Astronomy, University of Pennsylvania, 209 South 33rd Street, Philadelphia, PA 19104
[8] Department of Astronomy and Physics, Eastern University 1300 Eagle Road Saint Davids, PA 19087
[9] Department of Physics, University of California at Berkeley, Berkeley, CA 94270
[10] Steward Observatory, 933 North Cherry Avenue, Room N204 Tucson AZ 85721
[11] Department of Astronomy, Yonsei University, 134 Shinchon, Seoul 120-749, Korea
[12] Initiative in Innovative Computing, Harvard University, 60 Oxford St, Cambridge, MA 02138

The signatures we are searching for are brief reductions in flux from background stars due to occultations by small Kuiper Belt Objects (KBOs) and Extended Disk Objects (EDOs). The event rate and the spectrum of durations will be used to address the questions posed above. The occultation survey technique is uniquely suited to this task, since it is capable of detecting objects that are much fainter than the magnitude limit of any plausible direct survey (Bailey 1976). However, the occultation technique is difficult to implement in practice, so the project includes some important technology development goals. For more details on the occultation technique applied to searches for outer Solar System objects see Nihei et al. (2007), Cooray (2003), Cooray & Farmer (2003), Roques et al. (2006), Chang et al. (2007), and Roques et al. (2003). For an overview of the TAOS Project, see Lehner et al. (2006), Chen et al. (2007), and Alcock et al. (2003). For more information on the Kuiper Belt, see Jewitt & Luu (1993), Luu & Jewitt (2002), Bernstein et al. (2004), and Trujillo et al. (2001). For more information on the Extended Disk, see Brown et al. (2004), Kenyon & Bromley (2004), Morbidelli & Levison (2004), and Brasser et al. (2007).

In addition to the primary science goals stated above, a rapid response capability was implemented on the TAOS system to observe optical counterparts to Gamma Ray Burst (GRB) events reported to the GRB Coordinates Network[13] (GCN). This will be described in §6.7.

2. DESIGN CRITERIA

The TAOS system was designed to meet the following criteria:

- Make photometric measurements at a high sampling rate (5 Hz).

- Continuously monitor enough stars (∼1,000) to obtain a significant event rate.

- Low ($\lesssim$0.1 per year) false positive rate.

- Moderate cost.

- Credible result.

[13] `http://gcn.gsfc.nasa.gov/`, see also Barthelmy et al. (1998)

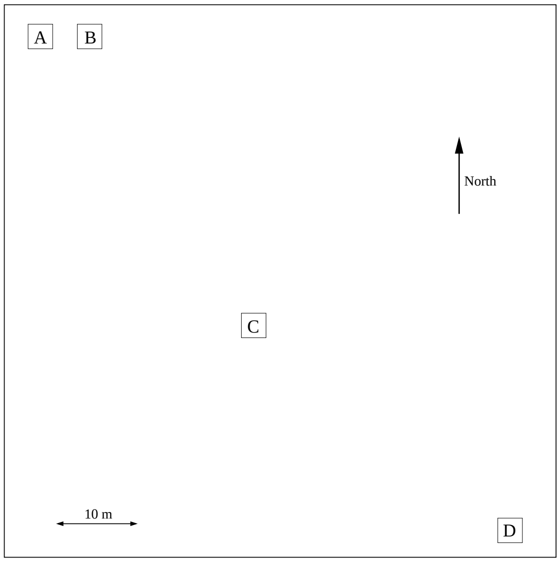

FIG. 1.— Layout of the four TAOS telescopes at Lu-Lin Observatory.

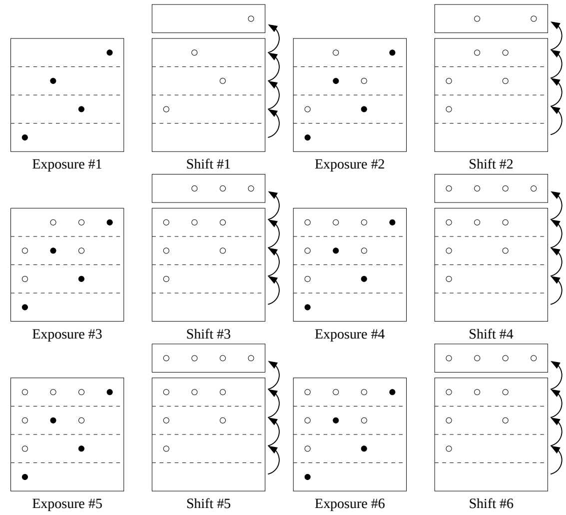

FIG. 2.— Illustration of zipper mode operation with the focal plane divided into four row blocks. Solid circles indicate actual stars, empty circles indicate locations of electrons after shifts. Note that after the fourth sequence of expose and shift operations, flux from all four stars is read out at each subsequent shift, although the flux from these stars was collected at different epochs.

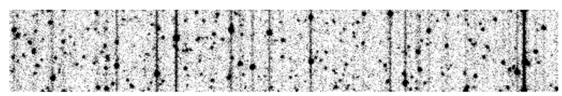

FIG. 3.— Example of a zipper mode image comprising a 512×76 subsection of a 2048×76 row block.

The rapid photometry is achieved by means of the innovative use of an otherwise conventional CCD camera (which will be described in §3). An adequate number of stars can be imaged by a modern CCD camera mounted on a small (50 cm), fast (F/1.9) telescope with a wide field of view (3□°). Moderate cost was achieved by using components that are readily available with a minimum of customization.

The low false positive rate is of great concern, and was a primary driver in the design. Our design goal was to be able to measure a rate of stellar occultations by KBOs of 1 event per 1,000 stars per year of observing time. We make $\sim 10^{10}$ photometric measurements per year, from which we want to derive less than one spurious occultation. The false alarm probability per observation must therefore be exceedingly small if the results of the experiment are to be interpreted with confidence. We control false alarms by requiring joint detections in an array of four independent robotic telescopes. These telescopes have separations ranging from 6 meters to 60 meters (see Figure 1). False positives of terrestrial or atmospheric origin (such as birds, aircraft, extreme atmospheric scintillation events, etc.) are removed by this requirement. False positives due to main belt asteroids can be eliminated by automated follow-up of detected events at a nearby, larger telescope. However, this would require a real-time analysis pipeline, which has not yet been implemented for this project. The telescopes are spaced far enough apart that scintillation events are unlikely to affect all of the telecopes. Note, however, that the telescopes are close enough that any occultation events would be detected by all four telescopes (see Nihei et al. (2007) for a detailed description of occultation events from objects in the Outer Solar System).

The multi-telescope design also allows us to address our last requirement. It would be difficult to credibly report on rare occultation events that were seen in only one telescope. The redundancy in the multi-telescope system greatly enhances the credibility of the reported result.

3. HIGH-SPEED PHOTOMETRY WITH ZIPPER MODE READOUT

The CCDs used for the TAOS project are described in §5.2. The devices are 2048×2052 e2v CCD42-40 chips. Each chip has two amplifiers, which allow for a combined readout rate of 1.8 MHz. It takes approximately 2.3 seconds to read out the entire frame, which makes our desired 5 Hz image cadence impossible without more than 90% dead time. To overcome this limitation, we have designed a novel method of operation, which we call *zipper mode*.

Zipper mode (see Figure 2) differs from conventional operation in the manner in which the CCD is read out. As with conventional operation, the telescope tracks the sky and stars are imaged onto the focal plane. However, instead of simply opening and closing the shutter for each exposure, the shutter is left open, and after 105 ms, a "row block" of 76 rows is read out. (The read out operation takes approximately 95 ms, so the readout time plus the exposure time is equal to our required sampling time of 200 ms.) This is followed by another "hold" of 105 ms, then another row block is read out. This cycle may be repeated for extended periods of time, possibly up to several hours. Note that after $2052/76 = 27$ row blocks are read out, photoelectrons from every star on the focal plane will be read out in each subsequent row block.

The ability provided by zipper mode to read at 5 Hz comes with a cost in signal-to-noise. This is due to two undesirable properties inherent to zipper mode, and any attempt to alleviate one of the problems exacerbates the other. First, photons from sky background are collected continuously during each hold and shift, while photons from a star are collected only during a single hold. Note

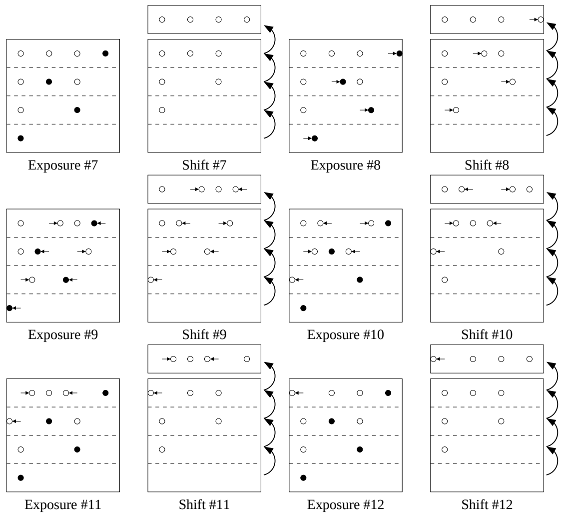

FIG. 4.— Continuation of zipper mode schematic shown in Figure 2, illustrating effect of tracking errors throughout a zipper mode run. In this illustration, the telescope drifts to the left during exposure #8, moving the stars to the right of the image. During exposure #9, the telescope moves too far back to the right, moving the stars to the left of the image. The arrows on the images indicate the displacements of the stars from their nominal positions. Note that the stellar flux that is read out in a row block is collected at different times, depending on where a star is located on the focal plane. Neighboring stars on a row block could therefore move in different directions from their nominal positions.

that with row blocks of 76 rows, the pixels in a single row block contain photoelectrons collected from a total of $2052/76 = 27$ holds. With a hold time of 105 ms and a sampling cadence of 5 Hz, the average recorded number of sky photoelectrons per pixel is thus a factor of $27 \times 200/105 = 51.4$ times brighter than it would be after a simple, 105 ms exposure. Second, it takes just over 1 ms to read a single row. Photons from stars are still collected during this time, meaning that stars will leave streaks as a row block is read out, as can be seen in Figure 3. Faint stars are particularly vulnerable to this effect of flux contamination by streaks of bright stars. One could conceivably reduce the sky background using row blocks with a larger number of rows, but this would reduce the effective exposure time relative to the readout time and reduce the measured stellar brightness relative to the brightnesses of the streaks.

We would ideally like the row block size to be an integral factor of 2052, the total number of rows on the CCD. (Stars near the edges of an image are missing a fraction of their flux, increasing uncertainty on the photometry not only of the edge stars but also of their neighbors. This effect is minimized if the row block size is an integral factor of the number of rows in the CCD.) We found the signal-to-noise ratio was highest when the read time was close to the exposure time, and the integral factor of 2052 meeting this requirement is 76 rows.

Because of the increased sky background, zipper mode works well only for relatively bright stars. On a dark night, adequate signal-to-noise ($\sim$7) can be achieved with a star of $V \sim 13.5$, which consequently is the faintest magnitude we plan to use in our occultation search.

This readout mode also requires accurate pointing and tracking throughout the duration of a zipper mode run, ideally to within a small fraction (~ 0.1) of a pixel. As shown in Figure 4, if there are significant oscillations in

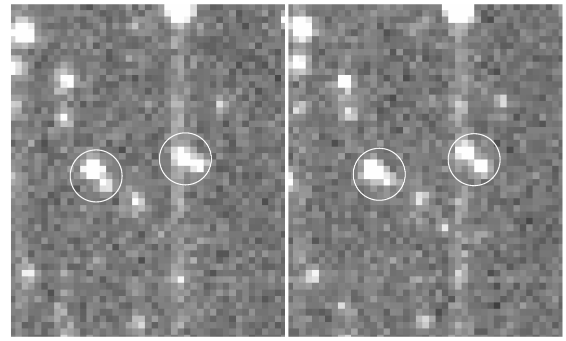

FIG. 5.— Two row block subsections taken at two different epochs. Note the two pairs of stars inside the circles. The two neighboring stars in the right circle are close together in the left image and have moved apart in the right (later) image. The two stars in the left circle moved closer together in the right image.

pointing error, then neighboring stars in a row block can move in different directions from their nominal positions over time. This can cause a significant reduction in signal-to-noise for closely neighboring stars in a row block due to varying blending fractions over time.

We did find significant oscillations in the tracking of the telescopes, as shown in Figure 5. Reducing the magnitudes of these oscillations required significant hardware improvements (see §5.1) and software modifications to the telescopes (see §6.5). These modifications were completed in September of 2005, so a large fraction of our first dataset suffered from this problem. This will be discussed in Zhang et al. (2008).

4. THE SITE

The telescopes are installed atop Lu-Lin Mountain (longitude 120° 50′ 28″ E; latitude 23° 30′ N, elevation 2850 meters), in the Yu Shan (Jade Mountain) area of Taiwan. The median seeing is 1.3″, with $\sim$100 clear nights per year. Most of the poor nights occur during typhoon season (May, June, and July). Since the beginning of 2005, TAOS has averaged $\sim$400 hours per year of actual observing, an average of 4 hours per clear night. High humidity is typically the reason the observing hours are limited on clear nights. Plans are currently being developed to start a new survey at a drier site, but TAOS will be operated at the current site for at least three more years.

5. THE HARDWARE

5.1. *The Telescopes*

The four identical telescopes (see Figure 6) were manufactured by Torus Technologies (now Optical Mechanics, Inc.). Each telescope has a 50 cm aperture imaging to a corrected Cassegrain focus at F/1.9. The corrected field-of-view comprises 3□°. Each system is controlled by an Oregon Micro Systems PC68 card. The HA and Dec axes are driven by friction wheels which are powered by Bearing Engineers Inc. Advanced Vector Servo systems. The axis positions are monitored by Renishaw RGH24 rotary encoders with 0.27 arc sec/step resolution. The secondary focus position is set by a screw drive powered by an Oriental Vexta PK245-03B motor controlled by an Intelligent Motion Systems IB462 bipolar stepping motor driver.

Each of the telescopes was delivered with severe mechanical defects which needed to be corrected to make the

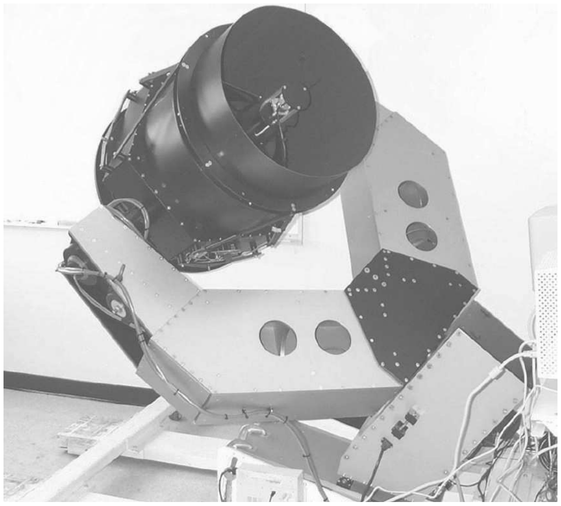

FIG. 6.— The TAOS B telescope.

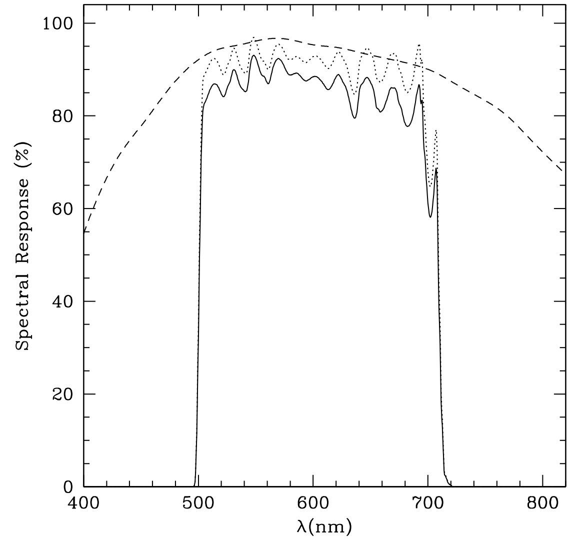

FIG. 7.— Spectral response of the camera system. The dashed line shows the quantum efficiency of the CCD, the dotted line shows the filter transmission, and the solid line shows the total spectral response. The quantum efficiency data for the CCD was obtained from the e2v website at `http://www.e2v.com`.

instruments sufficient for the requirements of the survey. First, the mechanical tolerances of a F/1.9 system are extremely tight. However, we found the mirrors would move by large amounts (the primary itself would move 4–5 mm as the telescope would slew from horizon to horizon, while the specified tolerance was < 50 μm). To correct this problem, the entire mirror support structures for both the primary and secondary mirrors were redesigned and refabricated by engineers at Lawrence Livermore National Laboratory. Second, the telescopes must accurately track for up to two hours, but we found the tracking accuracy limited by backlash in the drive system reduction gears and bad bearings in the friction wheel assembly. The friction wheel assembly was redesigned and refabricated by engineers at the Institute for Astronomy and Astrophysics at Academia Sinica in Taiwan, and the reduction gears were replaced with Bayside model PX-34-050-LB (50:1) devices. Finally, the primary mirror on the fourth telescope was found to have severe surface defects which distorted the point spread function beyond any reasonable shape and size. The mirror was repolished and resurfaced by the Space Optics Group at the Korea Research Institute of Standards and Science in Daejeon, South Korea, and it is now of sufficient quality for the TAOS survey. It should be noted, however, that the Point Spread Functions (PSFs) of all of the systems are a factor of two larger than was specified when procuring the telescopes, so the limiting magnitude of the system is roughly $M = 13.5$ instead of our target of $M = 15$, and we therefore are able to monitor fewer stars than originally planned. We are, however, still able to monitor a large enough number of stars at sufficient signal-to-noise that our results will still be very useful and will greatly increase our knowledge about the faint end of the Kuiper Belt.

The secondary focus system was also found to have poor resolution in positioning and significant backlash. To fix this, the entire secondary focus drive system was redesigned by engineers at Academia Sinica. A Renishaw RGH22 linear encoder with 0.1 μm resolution was added to each telescope to enable the secondary focus position to be accurately set to within 3 μm (the limiting resolution from the stepper motor and threading of the drive shaft). The encoders are equipped with limit switches to keep the secondary mirror from bottoming out against the support structure in one direction and completely unscrewing from the support structure in the other direction. The encoder system is also equipped with a magnetic reference mark to reproduce the home position within 0.1 μm, which is needed for the automatic focus control (see §6.4.7).

5.2. *The Cameras*

Each telescope is equipped with a thermoelectrically cooled Spectral Instruments Series 800 CCD camera employing a thinned, backside-illuminated e2v 2048×2052 CCD42-40 chip[14] The CCDs have 13.5 μm pixels, corresponding to a plate scale of 2.9 arc sec per pixel, and the total image area is 27.6 mm $\times$ 27.6 mm. There are two read channels, which work at a combined speed of 1.8×10^6 pixels per second. The gain of each amplifier is set to about 2.0 ADU/e$^-$, and the read noise is about 10 e$^-$. The cameras are operated at a temperature of -20° C, and the dark current is about 0.05 e$^-$/sec/pixel. Each CCD chip has the e2v mid-band coating, providing peak quantum efficiency of more than 93% and mean quantum efficiency over the spectral range we will employ of over 90%. Each camera has a custom-made filter (produced by Custom Scientific, Inc.) which provides more than 80% transmission between 500 nm $\lesssim \lambda \lesssim$ 700 nm. The quantum efficiency of the CCD and filter transmission curves are shown in Figure 7.

The camera was delivered with a chiller for the thermoelectric cooler, but we found this difficult to operate remotely. Since we do not need chilled water for our application the chillers were replaced with ITW Cooling Systems 2500SS welding coolers, which are simply water circulators with fan-cooled radiators. Each cooler is

[14] These chips are specified as 2048×2048, but there are four extra rows at the end of the CCD to act as a buffer for current leakage from the substrate. These rows must be read out in zipper mode as they are shifted with every other row. However, the current leakage is negligible at our 5 Hz image cadence, so we can use these extra rows as actual imaging area.

equipped with a GEMS 2659 flow switch relay, which will signal if the coolant flow stops for some reason.

5.3. *Weather Monitoring*

Accurate weather monitoring is clearly an important component in any robotic telescope system, especially at a site prone to rain and high humidity. Most of the weather information is monitored by two Vaisala WXT510 weather stations. Each weather station is controlled and read through a serial port interface by a small Linux workstation. The two systems are used for redundancy in case one of them fails. These weather stations provide information such as temperature, humidity, dew point, barometric pressure, and wind speed and direction.

While these weather stations are very robust and perform quite well, the relative humidity measurement is not very accurate when the relative humidity rises above 90%. This is an important parameter due to the fact that the humidity at Lu-Lin is often above this level. We solved the problem by installing a pair of Vaisala HMT337 humidity and temperature sensors. These devices are designed for high humidity applications, and specify an accuracy of $\pm 1.7\%$ in relative humidity (or more importantly, $\pm 0.3°$ C accuracy in the dew point). These devices are run by the same computers that control the weather stations.

Each telescope enclosure is also equipped with a Vaisala DRD11A Rain Detector to check for any precipitation. The sensors output an analog voltage proportional to the amount of moisture on the sensor surface, and these voltages are monitored by a computer in each enclosure by a serial analog to digital converter. The devices are extremely sensitive, and will trigger the closure of our enclosure lids immediately after the detection of a single droplet.

Temperatures of the various parts of each optical assembly (primary mirror, secondary mirror, support struts, etc.) are monitored by Picotech Technology Ltd. thermocouple sensors. These temperatures are compared to the dew point temperature so we can close our enclosure lids if the telescopes get cold enough for condensation to form, and to provide real time adjustments to our focus positions as the temperature changes. (This will be discussed in detail in §6.4.7.)

The weather parameters of most concern are precipitation, humidity, wind, and temperature. We would like the lids closed if there is any precipitation or if the humidity is high enough for condensation to form on the telescope components. Wind is primarily a concern because we do not want the lids open if the wind speed is high enough that the telescopes might get damaged, or if we are not able to close the lid at all (note that the lid effectively becomes a large sail during the opening and closing operations due to the clamshell design). Wind is also a concern because of the effect on the tracking accuracy of the telescopes. As discussed in §5.2, oscillations in the tracking accuracy due to wind will decrease the signal-to-noise ratio achieved by the system. Temperature monitoring is important because many of the telescope components (e.g. motor controllers) are not rated below certain temperatures.

We have therefore defined a set of alarm thresholds for these various weather parameters. If one of these parameters crosses a threshold, a "WEATH_BAD" alarm state is entered. If this alarm state is entered, the lids of all of the enclosures will immediately be closed automatically. In addition, we have defined a second set of thresholds which need to be crossed for the WEATH_BAD alarm state to be turned off. If a WEATH_BAD alarm state is entered, the weather parameters must be past the threshold values for 3 minutes before the alarm is turned off. This prevents the alarm from rapidly turning on and off when one of the parameters is hovering near the threshold. These thresholds are shown in Table 1.

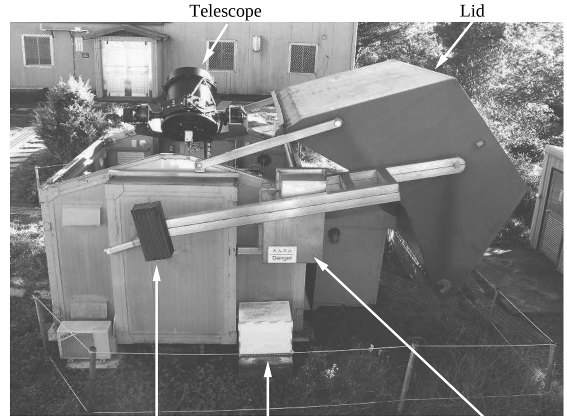

Fig. 8.— The enclosure for telescope TAOS A.

5.4. *The Enclosures*

The TAOS enclosures were designed to stand the hurricane force winds which accompany the 4 or 5 typhoons which typically move through the region every summer. The enclosure walls consist of two 1 mm thick steel plates separated by 5 mm of insulating foam and are supported by 10 cm × 10 cm steel beams. The working area is about 3 m × 3 m. The lids are of a counterweighted clamshell type design. They are made of polyurethane-filled fiberglass and were fabricated by the Aeronautical Research Laboratory of the Chungshan Institute of Science and Technology in Taiwan. Each lid is actuated by a ADLEE BM-370 brushless DC motor and a 1:400 worm reducer made by Shin Wei Ent Co. A custom control circuit is used to provide both manual operation and automated robotic operation through software. The time to open or close the lid is about one minute. In order to keep the lid operational during a power failure, the motor is powered by a SMR MCS1800 DC UPS made by Delta Electronics Inc.

Each enclosure is equipped with air-conditioning to keep the temperature of the telescope close to the anticipated night time temperature. This improves image quality by minimizing the temperature difference between the telescope components and the ambient temperature, and also minimizes the time used to find the best focus and focus change during the night.

A picture of the enclosure for telescope TAOS A is shown in Figure 8. Note that the telescope is installed high in the enclosure and is exposed to the outside elements when the lid is opened, making the telescope susceptible to wind and high humidity.

TABLE 1
Weather alarm parameters

Parameter	Alarm On Threshold	Alarm Off Threshold
DRD11A Voltage	< 2.5 V	> 2.8 V
Relative Humidity[a]	$> 95\%$	$< 94\%$
Dew point – temperature differential[b]	$< 1.0°$ C	$> 1.5°$ C
Average wind speed	> 20 km/hr	< 18 km/hr
Maximum wind speed[c]	> 30 km/hr	< 28 km/hr
Minimum temperature	$<$-5.0° C	$>$ -3.0° C

[a] Value reported by HMT337 dew point sensor.[b] Dew point value reported by HMT337 dew point sensor, temperature differentials calculated from HMT337 temperature reading and Picotech thermocouple measurements of telescope component temperatures.[c] Maximum wind speed measured over a 10 minute interval.

5.5. *The Robotic Observatory Control System*

In each enclosure, every subsystem other than the telescope and camera is controlled by a Sealevel Systems Model 8010 32 bit I/O card which is connected to a custom built interface box. These boxes are based on a design used by the ROTSE Survey (Akerlof et al. 2003), but the design has been extensively modified. The boxes control the power to the cameras, the camera coolers, and the telescopes. The boxes also monitor the limit switches on the telescopes, and will automatically cut the power to a telescope if one of the switches is tripped. This is done in hardware with a series of relay switches to ensure reliability. The chiller flow switches are also monitored by these systems, and the software will turn off the thermoelectric cooler on the CCD and cut the power to the chiller should the flow unexpectedly stop.

The lids are also controlled by these interface boxes. The lids are opened and closed by asserting 12 V signal lines to the lid controller boxes. The limit switches to the lids are also monitored, and once again a set of relay switches will automatically cut the power to the open/close line when the open/close limit switch is tripped.

Finally, each box is equipped with an ICS Advent WDT5 watchdog module. This module must be pinged by the I/O card once every second, or it will close a set of relay switches which will automatically cut the power to the telescope and close the lid. If the computer crashes or one of the control daemons should happen to die, the system will then be safe from any inclement weather which should arise before the system can be restarted.

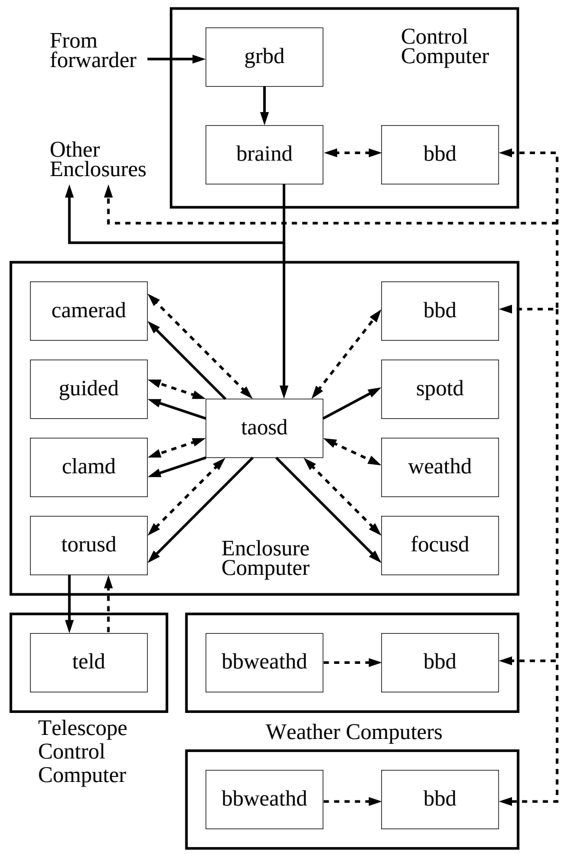

Fig. 9.— Schematic of the TAOS system control software. Solid arrows indicate control message bus, and dashed arrows indicate status message bus. See text for details.

6. THE SOFTWARE

The control software for the TAOS system is based on the control software used for the ROTSE Survey (Akerlof et al. 2003), however it has been extensively modified for TAOS. Each component of the system is controlled by a separate daemon. A schematic of the daemons and their communication paths can be seen in Figure 9, and a description of each daemon is given in the following subsections.

Each enclosure has a dual-CPU Pentium 4 computer to control all of the hardware described in the previous section, and a small PC104 computer to control the telescope via the OMS PC68 Motion Controller Card. The main control computer is located in the TAOS control building, which also houses two small computers to monitor the two sets of weather stations (see §5.3). All of the computers are running the Debian Sarge[15] distribution of Linux. Each of the main enclosure computers are running Linux kernel version 2.4.18 with the Kansas University Real-Time patch (KURT[16]) to provide microsecond timing resolution, which is important for synchronized zipper mode imaging at 5 Hz. The main control computer, weather station computers and telescope control computers are running kernel version 2.6.8. All four TAOS enclosures are connected to the control building by 1 Gbps fiber optic cable.

In order to provide accurate timing to the control computers (necessary for accurate telescope pointing and synchronized high-speed imaging), the clocks of all of the computers in the control system are synchronized via

[15] `http://www.debian.org`
[16] `http://www.ittc.ku.edu/kurt/`

ntp[17] to the control computer. The ntp server on control computer synchronizes to two ntp servers in Taiwan[18].

6.1. *Command and Status Message Passing*

All command and status information is passed from computer to computer via standard *inet* sockets using a custom message passing library. Command information is sent from the control computer directly to each enclosure computer.

Each computer has a System V shared memory area which contains all status information from each enclosure, the control computer, and the weather computers. We call the shared memory area the *bulletin board*, and the status information is kept up to date by the bulletin board daemon, *bbd*. There is an instance of *bbd* running on each computer in the local network, and once every second each instance of *bbd* updates every other instance with its local status information. Each daemon on the system thus has available up-to-date information on every other daemon running on the system.

6.2. *The Scheduler Daemon* braind

The scheduler has four internal states, described in Table 2. While the Sun is above the horizon, the scheduler is in the SHUTDOWN state. In this state the lid is closed and the telescope and camera are powered off. When the Sun goes below the horizon and the weather is good (see §5.3), the scheduler will enter the GRBMODE state. In this state, the lid will be opened and the telescope and camera will be powered on. No zipper mode occultation survey data will be collected in this state, however the system will respond to any GRB alerts that come in. (Zipper mode data are not so useful in twilight conditions due to the increase in sky background, however GRB follow-up data could be useful under this circumstance.) When the Sun goes below an elevation of $-18°$ (i.e. the sky is sufficiently dark), *braind* enters STARTUP mode, and it will subsequently commence zipper mode observations for the occultation survey. If any GRB alerts come in during a zipper mode run, *braind* will interrupt the observations and schedule follow-up observations for the GRB event. At the end of the evening, when the Sun rises above $-18°$, *braind* will go back into GRBMODE and will then only respond to GRB alerts. When the Sun rises above the horizon, *braind* will go back into SHUTDOWN mode for the day, and will close the lids and power down the telescopes and cameras.

If *braind* is in the GRBMODE or STARTUP states and at any time the weather should turn bad, the system will go into STANDBY mode and close the lids. If the weather becomes good again, *braind* will go into either the GRBMODE or STARTUP state, depending on the elevation of the Sun. If the weather is bad when the Sun sets, the system will go straight into the STANDBY state from the SHUTDOWN state. Conversely, if the system is in the STANDBY state at the end of the night when the sun rises, it will go into the SHUTDOWN state.

Every evening after sunrise and sunset, *braind* will schedule a set of dark images to be taken on each camera. At sunset, this happens 300 seconds after *braind* enters the GRBMODE state to give the camera ample time to cool down. At sunrise, the darks images are taken after the lids are closed but before the system enters the SHUTDOWN state. Each series of dark images comprises a set of 20 stare mode dark images with 1 second exposures, and a series of 10 zipper mode dark images with the standard zipper mode parameters (5 Hz sampling, blocks of 76 rows, and 32 row blocks per FITS file).

[17] Network Time Protocol. See `http://www.ntp.org/`.

[18] tick.stdtime.gov.tw, stdtime.sinica.edu.tw

6.3. *The Weather Daemon* bbweathd

The weather stations and dew point sensors described in §5.3 are read by two instances of *bbweathd*, one instance for each set of one weather station and one dew point sensor. This daemon (as the name implies) simply reads both devices and publishes the information on the bulletin board for other software components to monitor. In addition, *bbweathd* will check the measured weather parameters against a set of limits, and set an alarm if adverse weather is detected. This alarm state is also written to the bulletin board for other daemons to monitor.

6.4. *Control Daemons*

In addition to the instance of *bbd* described above, each enclosure computer runs a set of eight control daemons, each dedicated to a particular hardware component (or set of components) or high level control task. These daemons are described in the following subsections.

6.4.1. *The Master Control Daemon* taosd

Every daemon running on the enclosure computer is a child of *taosd*. This daemon is responsible for forwarding commands from *braind* to the appropriate child daemon, and for monitoring the status of each of the children and passing the status information on to the local instance of *bbd*. Each child daemon has a dedicated System V shared memory area which is used to pass command and status information to and from *taosd*. This daemon will automatically send commands to certain daemons based on the status information of other daemons (e.g. it will close the lid if adverse weather is detected).

6.4.2. *The Watchdog Daemon* spotd

. This simple daemon is responsible for pinging the watchdog module in the observatory control interface box described in §5.5. The daemon is designed to run independently of the rest of the daemons on the system to enable manual control (e.g. so the lid can be opened manually without the rest of the software running), however when *taosd* is running, a simple "I'M ALIVE" command is expected from *taosd* at a rate of 1 Hz. If this command times out, *spotd* will die, the telescope will be stopped and the lid will automatically be closed. Thus if *taosd* should crash or otherwise be hung up for some reason, or if the enclosure computer itself should crash, the system will automatically go into a safe mode.

6.4.3. *The Local Weather Daemon* weathd

While general weather information is monitored by *bbweathd* as described above, a local weather daemon *weathd* runs on each enclosure computer as well. This daemon has three tasks. First, *weathd* monitors the Vaisala precipitation sensors described in §5.3. Second, it monitors the local copy of the *bbweathd* information

TABLE 2
SCHEDULER STATES

State	Sun Elevation	Weather Status	Lid Position	Telescope and Camera Power
SHUTDOWN	$\geq 0°$	good or bad	closed	off
GRBMODE	$< 0°$	good	open	on
STARTUP	$< -18°$	good	open	on
STANDBY	$< 0°$	bad	closed	on

on the bulletin board. If precipitation is detected or *bbweathd* reports adverse weather, a flag is set in the *weathd* shared memory segment which will instruct *taosd* to abort any current observations and close the lids. Finally, *weathd* monitors the telescope strut and mirror temperatures read by the thermocouple sensors attached to the telescope (see §5.1), and compares these temperatures to the dew point reported by *bbweathd* to see if the lid needs to be closed to prevent condensation on the telescope.

6.4.4. *The Telescope Command and Status Daemon* torusd

The telescope is directly controlled by a small PC104 computer via an OMS PC68 motion controller card, and communication between the main enclosure computer and the PC104 computer is handled by *torusd*. This daemon connects to the telescope control daemon *teld* (see §6.5) over a set of four inet sockets, one for pointing and tracking control, one for the focus control, one for status information and one for miscellaneous control commands.

6.4.5. *The Guide Daemon* guided

While we have greatly improved the pointing and tracking capabilities of the system through both software and hardware modifications, we found the pointing was still inadequate for the survey. Accurate pointing (within 0.3 arc sec) must be maintained throughout an entire zipper mode run, which can last as long as 2 hours. As discussed in §5.2, poor tracking can significantly decrease the signal-to-noise performance of the system, so it is desirable to keep the tracking as accurate as possible. While many surveys have a separate guiding imager, TAOS has the advantage that images are collected at a high rate, and we use this feature to enable our guiding system.

The guide daemon runs in two modes. During the initial pointing phase, we point the telescope to a field center and take a stare mode image. This image is analyzed to find the actual RA and Dec of the image center, and a pointing offset is calculated. A pointing adjustment command is sent to *torusd*, and the process is repeated until the center of the image is within 0.1 pixels of the actual field center. In this way, at the beginning of a zipper run, all four telescopes are pointing to within 0.3 arc sec of the target field center.

The image analysis routine makes heavy use of the standard software packages *SExtractor* (Bertin & Arnouts 1996) and *wcstools* (Mink 2006) used in conjunction with the USNO-B1.0 catalog (Monet et al. 2003). First, after an image is taken, the *wcstools* utility *imwcs* is run to find the World Coordinate System (WCS) keywords to transform RA and Dec to pixel coordinates. Second, *SExtractor* is run to find objects in the image. Third, the *SExtractor* output is used with the *wcstools* utility *immatch* to match the objects found by *SExtractor*. Finally, a set of polynomials (Malumuth & Bowers 1997) are fit to the data to convert from x and y, the pixel coordinates of each matched star calculated from the WCS coefficients, to x_p and y_p, the actual centroid locations reported by *SExtractor*. The polynomials are of the form

$$\begin{aligned} x_p = & C_0 + C_1x + C_2y + C_3x^2 + C_4xy + C_5y^2 \\ & + C_6x^3 + C_7x^2y + C_8xy^2 + C_9y^3 \\ y_p = & D_0 + D_1x + D_2y + D_3x^2 + D_4xy + D_5y^2 \\ & + D_6x^3 + D_7x^2y + D_8xy^2 + D_9y^3, \end{aligned}$$

where C_i and D_i are the fit coefficients. After the fits are complete, these distortion coefficients and WCS keywords are used to calculate the RA and Dec of the center of the image, which is then used to calculate the pointing offset. The pointing offset is written to the *guided* shared memory status segment, which is then read by *taosd* and passed to *torusd* as a pointing adjustment command.

The second *guided* mode is the tracking mode. At the end of the initial pointing phase, 20 guide stars are selected from the stare mode image. The stars are selected on criteria including moderate brightness (i.e. bright enough to have good signal-to-noise characteristics but not so bright as to leave significant streaks in the zipper images), isolated (no close neighbors in zipper mode images), and they should be spread out through the image so the entire focal plane is well sampled. Note that a set of 32 consecutive row blocks is typically written to each FITS file, so there are effectively 640 guide stars in each image. Every 30 seconds, the last FITS image that was written to disk is analyzed. *SExtractor* is run on the image, and the centroids of the guide stars are found and compared with the original values. A pointing correction is calculated and written to the *guided* shared memory status segment, which in turn is read by *taosd* and passed as a pointing adjustment command to *torusd*. We find that the inherent tracking of the system is sufficient that the pointing drifts by much less than 0.1 pixel in the 30 second guiding update period, and *guided* is thus able to keep the pointing correct throughout an entire zipper mode run of up to two hours in duration.

The guide daemon also monitors image rotation throughout the course of a zipper run. Taiwan suffers from frequent earthquakes which can disrupt the polar alignment of the telescopes. We can thus learn in real time if the telescopes need realignment. Furthermore, *guided* reports the visibility conditions throughout the duration of a zipper mode run by monitoring the star count. Each time a zipper mode FITS file is analyzed for tracking adjustments, *SExtractor* reports the number of stars to which it can fit a standard PSF. The star count is compared to the number of stars found at the beginning of the zipper mode run to know how the observing conditions vary throughout the run. In our fully automated observing mode, *taosd* will interrupt observations if the star count drops significantly. This usually occurs due to incoming clouds, or if the seeing degenerates due to humidity or focusing problems. This real-time image quality analysis helps optimize our data collection as we can interrupt a zipper mode run and refocus the telescope if necessary.

6.4.6. *The Lid Control Daemon* clamd

The lid is opened and closed by a relatively simple daemon *clamd*. This daemon will assert an open or close signal to the lid controller on command, and monitor the open and close limit switches on the lid. The open and close signals are lowered when the appropriate limit switch is hit. The daemon will also set an alarm if the open or close operation times out, and this alarm will alert someone to fix the problem manually.

6.4.7. *The Focus Control Daemon* focusd

The focus control daemon *focusd* has two tasks. The first is to analyze images taken during a *focus sequence* to determine the ideal focus position. A focus sequence consists of a series of one second exposures taken with secondary mirror at different focus positions. A total of 17 images are acquired while moving the focus position by 15 μm steps. A 1k×1k sub-image from the center of the focal plane is analyzed using *SExtractor* to find the average Full Width Half Maximum (FWHM) of each star in the image, and the focus position and medium FWHM are logged internally. After all of the images have been collected and analyzed, the FWHM data are fit to two straight lines, one line on each side of the point with the minimum FWHM. These fits are then used to calculate the best focus position, which is then entered into a database along with the telescope component temperatures (reported by *weathd*) and zenith angle of the telescope (reported by *torusd*).

The second function of the focus daemon is to monitor the telescope component temperatures and zenith angle throughout a zipper mode run and to look up the ideal focus position in the database. If the ideal focus position changes, the new position is written to the *focusd* shared memory status segment, where it is read by *taosd* and passed on to *torusd* as a focus adjustment command.

6.5. *The Telescope Control Daemon* teld

The system originally used the *telescoped* program from the OCAAS[19] software package to control the telescope. However, we found two problems with this code that led us to the decision to write a completely new software package. First, the pointing model used by OCAAS did not accurately represent the pointing actually realized with the system. The residuals between the model and the true pointing were often as high as 10 arc minutes. Second, the software was written such that everything was controlled in a single main loop, and we found that the timing of the loop would vary and that this would introduce slight, but significant oscillations in the tracking. This had the effect of increasing the noise in our lightcurves, as discussed in §5.2.

The replacement daemon, *teld* is a multi-threaded program with separate threads dedicated to telescope control, focus control, status reporting, and master control (i.e. a parent thread to monitor the children). In addition, when tracking a field a new thread is spawned to control the telescope tracking directly. This thread runs with an elevated scheduling priority to keep the timing of the control loop accurate. Implementing a multi-threaded solution to the telescope control also required rewriting the driver for the PC68 motion controller card to make it thread safe. This was done by simply adding a semaphore to the driver which is raised whenever the card is accessed.

The daemon makes use of the SLALIB Positional Astronomy Library[20] to convert to and from J2000 RA and Dec to observed HA and Dec ($h_{\rm obs}$ and $\delta_{\rm obs}$). A custom pointing model derived from that used by the TPOINT software package[21] is used to convert $h_{\rm obs}$ and $\delta_{\rm obs}$ to actual encoder angles (x for the hour angle encoder and y for the declination encoder). The pointing model used is:

$$
\begin{aligned}
h_1 &= h_{\rm obs} - {\rm TF}\cos\theta_{\rm lat}\sin h_{\rm obs}/\cos\delta_{\rm obs} \\
\delta_1 &= \delta_{\rm obs} - {\rm TF}(\cos\theta_{\rm lat}\cos h_{\rm obs}\sin\delta_{\rm obs} \\
&\quad - \sin\theta_{\rm lat}\cos\delta_{\rm obs}) \\
&\quad - {\rm KZ}\cos\delta_{\rm obs} - {\rm MZ}\sin\delta_{\rm obs} \\
&\quad - {\rm FO}\cos h_{\rm obs} \\
x &= -h_1 + {\rm CH}\sec\delta_1 + {\rm NP}\tan\delta_1 + \\
&\quad ({\rm ME}\sin h_1 - {\rm MA}\cos h_1)\tan\delta_1 + {\rm IH} \\
y &= \delta_1 - {\rm ME}\cos h_1 - {\rm MA}\sin h_1 - {\rm ID}
\end{aligned}
$$

where h_1 and δ_1 are temporary variables, $\theta_{\rm lat}$ is the geodetic latitude of the site and the ten pointing model coefficients are described in Table 3.

After implementing *teld*, we found the typical differences between the calculated and true positions to be less than 10 arc seconds. Used in conjunction with *guided*, we found that we can track to well within 0.3 arc sec for durations up to at least two hours.

We also implemented an automatic pointing model feature to the system. A set of 40 images is taken at a grid of locations on the sky, and the images are analyzed by *guided* to find the actual RA and Dec of the centers of the images. The subsequent arrays of RA, Dec, x, y, and epoch are fit using the *amoeba* fitting routine adapted from Press et al. (1994). This works much faster than the OCAAS method of adjusting the pointing by hand until a catalog star is centered on the image and repeating several times, especially when it must be done to all four telescopes several times a year (e.g. after earthquakes). This also allows a new pointing model to be created remotely and automatically.

6.6. *Collection of Zipper Mode Data*

When the system is in STARTUP mode, *braind* will schedule a series of zipper mode *runs*. At the start of a run, *braind* will choose a standard TAOS field based on criteria such as distance from the ecliptic plane and

[19] Observatory Control and Astronomical Analysis System, see `http://www.clearskyinstitute.com/`

[20] `http://star-www.rl.ac.uk/`

[21] `http://www.tpsoft.demon.co.uk/`

TABLE 3
Pointing model coefficients

Coefficient	Description
IH	Hour angle home switch position
ID	Declination angle home switch position
CH	Collimation error
NP	Non-perpendicularity of h and δ axes
MA	Azimuthal polar alignment error
ME	Elevation error in polar alignment
TF	Tube flexure
FO	Fork flexure
KZ and MZ	First order correction to declination encoder error

distance from zenith. The scheduler will then instruct *torusd* to point all of the telescopes at the field center. Each telescope will then undergo a focus sequence (see §6.4.7) and set the secondary focus to the best position. Once this is completed, each telescope will undergo a pointing correction, as described in §6.4.5. Once all of the telescopes are pointing correctly, a set of three 1 second stare mode images are acquired for diagnostic purposes. Next, the zipper mode sequence is started. Each camera system is sent a start time by *braind*, and when the start time is reached, the shutters are opened and zipper mode readout is commenced. This 5 Hz readout process continues for a total of 90 minutes (as long as the weather remains good and no GRB alerts are received). Throughout the duration of the run, *guided* will keep the telescope pointed correctly. At the end of the run, a second set of three diagnostic stare mode images are acquired, also with 1 second exposures. Finally, a sequence of 1 second stare mode images is acquired with pointing offsets of 0.8° on a 3×3 grid about the center of the field. This provides an effective mosaic image of 11□° centered on the field, which is also used for diagnostic purposes.

Throughout a zipper mode run, *braind* will monitor the results of each command and the status of each daemon. If an error occurs, *braind* will attempt to recover by restarting any software that needs it and, if necessary, reinitializing the zipper mode run. If *guided* reports bad observing conditions, the zipper run will be aborted. A new field may be selected at this time based on the scheduling criteria discussed above, and if so *braind* will instruct the telescopes to point to the new field. In any case, the system will then undergo a new focus sequence to refocus the telescopes. If the weather is cloudy, this step will fail due to the lack of stars in the images. In this case, the system will wait for 300 seconds and reattempt the focus sequence. This step will be repeated until the weather clears. If the cloudy weather lasts long enough, a new field may be selected by *braind* in the meantime.

Every morning, all of the FITS images from the previous evening (typically about 40 GB per telescope on a clear night) are archived to a local RAID server in the main control building. Once every month or so, the data are copied to a set of hard drives which are physically brought to Academia Sinica. The data are copied to a local data server, and then transfered to the Taiwan National Center for High-Performance Computing[22] for backup to tape. Finally, the data are copied over the internet to a second RAID server located at National Central University. We then have three copies of the data in separate locations for secure, redundant data storage. The data are subsequently analyzed on using two computer clusters (at Academia Sinica and National Central University) with a custom photometry package that will be described in Zhang et al. (2008).

6.7. *The GRB Alert Response System*

The TAOS GRB response system consists of two components, the *forwarder* and the GRB daemon *grbd*. The *forwarder* simply listens to a socket connected to the GCN, and passes the information on to *grbd*. The purpose of the *forwarder* is to run on a machine with a more reliable internet connection than that available at Lu-Lin Observatory. If the internet connection to Lu-Lin is down, the *forwarder* still receives the GCN packet and keeps trying to forward the packet to *grbd* until it succeeds. We currently run the *forwarder* on a computer at the Institute for Astronomy and Astrophysics at Academia Sinica in Taipei.

When *grbd* receives a GCN alert packet from the *forwarder*, it parses the message and determines whether the reported event can be followed up by the TAOS system. If the GRB event is observable, *grbd* calculates an observation schedule and passes the request on to *braind*, which will interrupt any zipper mode operations and schedule the GRB follow-up observations.

TAOS has the advantage of multiple telescopes operating at the same site, which makes it possible to use different exposure times for the same event. Our observing scheme is optimized to have at least one telescope looking for fine structure in the light curves of bright events with short exposures, and two telescopes taking longer exposures for sensitivity to fainter afterglows. In the future, we may schedule one telescope to observe in zipper mode at 5 Hz to look for very bright and rapidly varying transients. To date, 10 GRB alerts were responded to by the TAOS system. The results of these observations will be described in detail in Wang et al. (2008).

7. SYSTEM PERFORMANCE

All telescopes were delivered with strong spherical aberrations over the whole field as well as significant astigmatism in the corners of the images. These problems were minimized by improved optical alignment after the telescope modifications discussed in §5.1, however the poor quality of the optical elements limited our attempts to improve the image quality. The best PSFs now range from 1.6 pixels (4.6 arc sec) in the center of the image to 2.5 pixels (7.3 arc sec) in the corners. We have designed a

[22] `http://www.nchc.org.tw/`

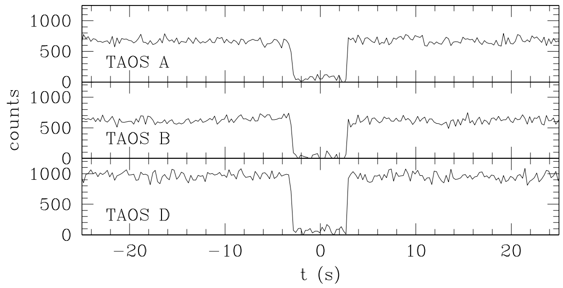

FIG. 10.— Lightcurves from three TAOS telescopes of the occultation of the star TYC 076200961 ($V = 11.83$) by the asteroid Iclea ($V = 14.0$, diameter = 97 km) at UTC 12:35 February 6, 2006.

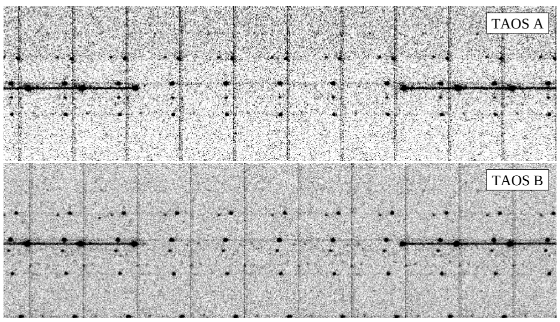

FIG. 11.— Zipper mode sub-images from telescopes TAOS A and TAOS B of the occultation of the star HIP 050535 ($V = 8.46$) by the asteroid Klemola ($V = 15.7$, diameter = 31 km) at UTC 12:10 June 5, 2004. Each sub-image is an exposure of 0.25 seconds, with time increasing to the right. The vertical lines visible in each set of images are caused by a slight excess in dark current from the CCD substrate, and indicate the boundaries of the row blocks. These images were taken before *guided* was implemented, so the two telescopes have different pointing offsets and the occulted star is in a different location in the row block.

Hartmann-Shack device to routinely check on the optical performance of telescopes.

To test the overall performance of the system we have observed several predicted asteroid occultations. Figure 10 shows the lightcurves of the occultation of the star TYC 076200961 ($V = 11.83$) by the asteroid *Iclea* ($V = 14.0$, diameter = 97 km) at UTC 12:35 February 6, 2006. The event was observed by operating the three functioning telescopes at 4 Hz, and the event, which lasted approximately 6 seconds, is clearly visible, indicating that the system is indeed capable of accurate, high-speed imaging. Figure 11 shows a series of zipper mode images of the occultation of the star HIP 050535 ($V = 8.46$) by the asteroid *Klemola* ($V = 15.7$, diameter = 31 km) at UTC 12:10 June 5, 2004. This was a short duration event, lasting only 1.3 seconds.

These asteroid occultation events clearly illustrate that the TAOS system is capable of detecting short duration occultation events with multiple telescopes. The system has been collecting data for over three years with three telescopes, and the fourth telescope has recently come online. Since February of 2005, we estimate TAOS has made over 5×10^{10} individual photometric measurements. Observations are continuing, and we plan to run the survey for at least three more years.

This work was supported in part by the National Science Foundation under grant AST-0501681 and by NASA under grant NNG04G113G, both at the Harvard College Observatory. The work at NCU is supported by the grant NSC 96-2112-M-008-024-MY3. SLM's work was performed under the auspices of the U.S. Department of Energy by Lawrence Livermore National Laboratory in part under Contract W-7405-Eng-48 and by Stanford Linear Accelerator Center under Contract DE-AC02-76SF00515. YIB acknowledges the support of Korea Astronomy and Space Science Institute. KHC's work was performed under the auspices of the U.S. Department of Energy by Lawrence Livermore National Laboratory in part under Contract W-7405-Eng-48 and in part under Contract DE-AC52-07NA27344. MJL wishes to thank Jeff Klein at the University of Pennsylvania for valuable advice regarding the system hardware development.

REFERENCES

Akerlof, C. W., et al. 2003, PASP, 115, 132, arXiv:astro-ph/0210238

Alcock, C., et al. 2003, Earth, Moon, Planets, 92, 459

Bailey, M. E. 1976, Nature, 259, 290

Barthelmy, S. D., et al. 1998, in American Institute of Physics Conference Series, Vol. 428, American Institute of Physics Conference Series, ed. C. A. Meegan, R. D. Preece, & T. M. Koshut, 99–+

Bernstein, G. M., et al. 2004, AJ, 128, 1364

Bertin, E., & Arnouts, S. 1996, A&AS, 117, 393

Brasser, R., Duncan, M. J., & Levison, H. F. 2007, Icarus, 191, 413

Brown, M. E., Trujillo, C., & Rabinowitz, D. 2004, ApJ, 617, 645

Chang, H.-K., et al. 2007, MNRAS, 378, 1287, arXiv:astro-ph/0701850

Chen, W. P., et al. 2007, in IAU Symposium, Vol. 236, IAU Symposium, ed. G. B. Valsecchi & D. Vokrouhlický, 65–68

Cooray, A. 2003, ApJ, 589, L97, astro-ph/0304396

Cooray, A., & Farmer, A. J. 2003, ApJ, 587, L125

Jewitt, D., & Luu, J. 1993, Nature, 362, 730

Kenyon, S. J., & Bromley, B. C. 2004, Nature, 432, 598

Lehner, M. J., et al. 2006, Astron. Nachr., 327, 814

Luu, J. X., & Jewitt, D. C. 2002, ARA&A, 40, 63

Malumuth, E. M., & Bowers, C. W. 1997, in The 1997 HST Calibration Workshop with a new generation of instruments /edited by Stefano Casertano, Robert Jedrzejewski, Charles D. Keyes, and Mark Stevens. Baltimore, MD : Space Telescope Science Institute (1997) QB 500.268 C35 1997, p. 144., ed. S. Casertano, R. Jedrzejewski, T. Keyes, & M. Stevens, 144–+

Mink, D. 2006, in ASP Conf. Ser. 351: Astronomical Data Analysis Software and Systems XV, ed. C. Gabriel, C. Arviset, D. Ponz, & S. Enrique, 204–+

Monet, D. G., et al. 2003, AJ, 125, 984, astro-ph/0210694

Morbidelli, A., & Levison, H. F. 2004, AJ, 128, 2564, arXiv:astro-ph/0403358

Nihei, T. C., et al. 2007, AJ, 134, 1596, arXiv:astro-ph/0703460

Press, W. H., et al. 1994, Numerical Recipes in C (Cambridge University Press)

Roques, F., et al. 2003, ApJ, 594, L63

——. 2006, AJ, 132, 819

Trujillo, C. A., et al. 2001, AJ, 122, 2740

Wang, J.-H., et al. 2008, in preparation

Zhang, Z.-W., et al. 2008, in preparation